International Journal of Engineering Trends and Technology
ISSN: 2231 – 5381 / https://doi.org/10.14445/22315381/IJETT-V70I6P223

Volume 70 Issue 6, 209-220, June 2022

Original Article

Characterization of Proposed Iterative Hyperbolic Localization Solution using Statistical Studies

Eswara Chaitanya Duvvuri[1], Vinod Kumar Minchula[2], Suresh Kumar Pittala[3], Sasibhushana Rao Gottapu[4]

[1,3]*Department of E.C.E., R.V.R & J.C College of Engineering, Guntur, India.*
[2]*Department of E.C.E., Chaitanya Bharathi Institute of Technology, Hyderabad, India.*
[4]*Department of E.C.E., Andhra University College of Engineering, Visakhapatnam, India.*

[1]d.e.chaitanya@gmail.com

Received: 10 April 2022 Revised: 07 June 2022 Accepted: 16 June 2022 Published: 29 June 2022

Abstract *- Localizing a radiating source is a rapidly growing research area with diverse applications in fields ranging from defence and industrial automation to agriculture. Apart from being used in areas not accessible to G.P.S., this system can be deployed to attend to distress signals. This paper proposes an iterative hyperbolic localization solution, and error analysis is carried out. The error scatters plot comparing errors in estimated x, y, and z locations are generated to conduct an error analysis of the chosen algorithm. Source locations are simulated near and far from a chosen square sensor geometry, and a novel characterization of the algorithm is proposed using statistical accuracy measures like Circular Error Probability (C.E.P.), 2DRMS, and Spherical Error Probable (S.E.P.). The figure of merit used here is the ratio of C.E.P. to the source distance, and from the result analysis, it can be inferred that the proposed algorithm performs well irrespective of the source distance.*

Keywords *- Hyperbolic, T.D.O.A., Localization, C.E.P., G.D.O.P.*

1. Introduction

Advances in electronic warfare have become the prime focus for many governments, and funds amounting to billions are being spent on research that aids the development of the latest technologies in the defense sector and applied fields [1]. Radio source localization can be especially useful in responding to remote areas' distress signals. Multilateration or Hyperbolic localization using Time Difference of Arrival (T.D.O.A.) is a nonlinear technique. There is always scope for improvement in algorithms that try to provide the closest approximation to the true source location.

This paper aims to characterize the proposed algorithm's performance using Circular Error Probability (C.E.P.) analysis for localization of near and far-field unknown radiating sources. The content of this paper is presented in 7 sections. The choice of measurement technique is discussed in Section 2. The hyperbolic multilateration and problem formulation are introduced in the third section. The fourth section details the steps in computing localization solutions using the proposed algorithm. Section 5 presents the working methodology and steps in algorithm evaluation and introduces C.E.P. Section 6 carries out result analysis. Finally, in section 7, the conclusions relevant to the following discussion are presented.

2. Choice of Measurement Technique

Accurate position determination of an unknown radiating source (viz. radar, aircraft) using a source localization system is crucial to determining a country's capabilities in electronic warfare. Several factors must be considered for developing a localization system over any geographic location. They are as follows: (i) operating medium (homogeneous and non-homogeneous), (ii) measurement technique, (iii) environmental effects on the measurements (water salinity, density, multipath, etc.), (iv) source to sensor/receiver geometry, (v) localization algorithm, etc.

A predominant factor that affects the performance of a localization system is the choice of the measurement technique. Improper selection of measurement techniques results in bad estimates of the true position. The various measurement techniques used in positioning, i.e., Time of Arrival (TOA), T.D.O.A., Received Signal Strength (RSS), and Direction of Arrival (D.O.A.), provide positional information by measuring the arrival time, distance, power, and direction of the received signal.

The TOA, T.D.O.A., and RSS techniques offer definite and precise position estimates when operating in a homogeneous medium (e.g., air) under explicit system conditions. The D.O.A. technique uses measurements independent of the signal's time and strength, making it suitable for source localization in a non-homogeneous medium. The TOA and T.D.O.A. measurement techniques make use of the travel or/and arrival time of the signal in determining the unknown position. T.D.O.A. techniques are especially suited when the source is localized unknown. An attempt is made to compare the performance of TOA and T.D.O.A. measurement techniques. For this purpose, real-time data is used to implement TOA and

T.D.O.A. techniques for the Global Positioning of an unknown object. The data is obtained from a Dual Frequency G.P.S. receiver located at Andhra University, Visakhapatnam, throughout 23hrs 56 mins. To solve the system of nonlinear range difference equations for T.D.O.A. and range equations for TOA, the Least Squares estimator is used. Source localization of an unknown radiating source, U obtained with TOA measurements, is illustrated in Figure 1.

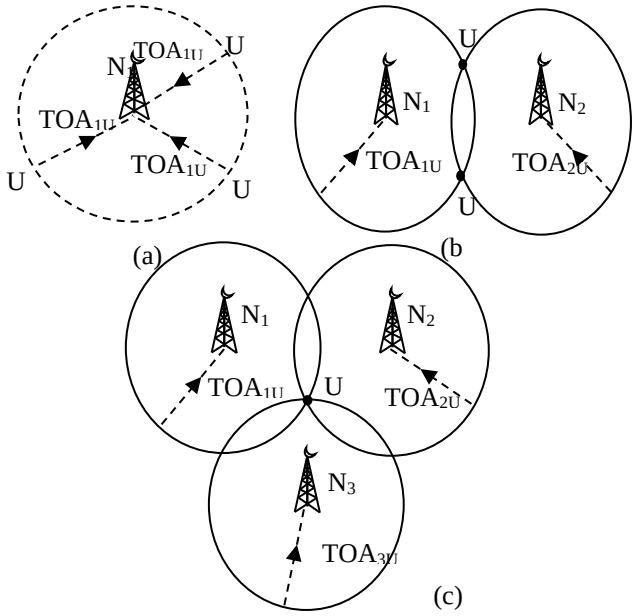

Fig. 1 Source localization using TOA measurements
a) Infinite possible solutions b) two possible solutions
c) ambiguity resolved in source position.

It is evident from Figure 1a that with one TOA measurement (TOA_{1U}), the location of the source 'U' can be anywhere on the circle. Combined with another TOA measurement (TOA_{2U}), it leads to an ambiguity in the source location, as shown in Figure 1b. Upon considering TOA_{3U}, this ambiguity is resolved as depicted in Figure 1c. Hence, a minimum of three TOA measurements are required for source localization with receivers placed in a coplanar configuration, as shown in Figure 1c. The same would need four TOA measurements for a non-coplanar receiver arrangement (i.e., Spherical form instead of circles) [2].

However, though the Time of Arrival technique has gained traction in recent years, so far, its usage has been limited to G.P.S. only due to the following constraints:

- The receiver and source clocks must be precisely time-synchronized.
- The source transmitted signal needs to be time stamped with signal initiation time which is used for TOA computation at the receiver.
- TOA measurements are not available from an unknown source

For TOA measurements, the variation in receiver position error with time is shown in Figure 2. For TOA measurements, the mean errors in receiver X, Y, and Z position coordinates are 54.2m, 147.7m, and 47.4m, respectively [3].

For T.D.O.A. measurements, the variation in receiver position error with time is shown in Figure 3. The mean errors in receiver X, Y, and Z position coordinates are 51.7m, 104.2m, and 35.3m, respectively [3].

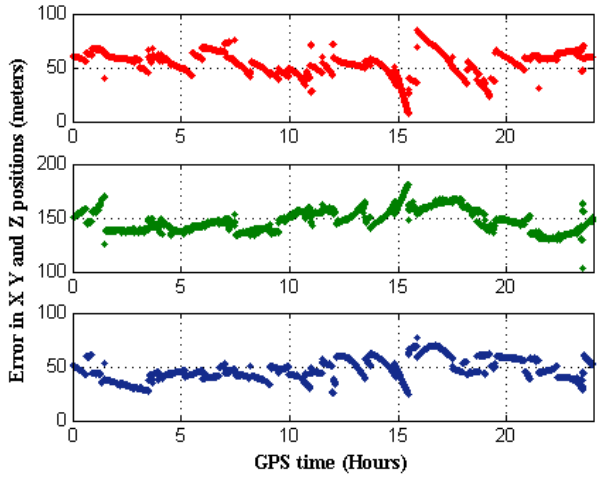

Fig. 2 Error in G.P.S. receiver position estimate using TOA measurements

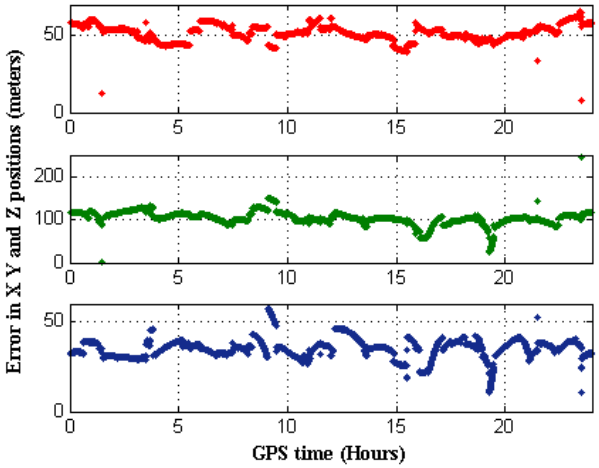

Fig. 3 Error in G.P.S. receiver position estimate using T.D.O.A. measurements

From the above results, it can be suggested that the T.D.O.A. performs better when compared to TOA. The TOA and T.D.O.A. measurement techniques are well suited for G.P.S. and source localization applications and are often used for long and medium-range positioning applications. While D.O.A. is an optimal measurement technique for non-homogeneous source localization applications (e.g., underwater localization and capsule endoscopy), the RSS technique is used for homogeneous and short-range source localization applications in multipath environments.

3. Hyperbolic Localization and Problem Formulation

A typical source localization system is shown in Figure 4.

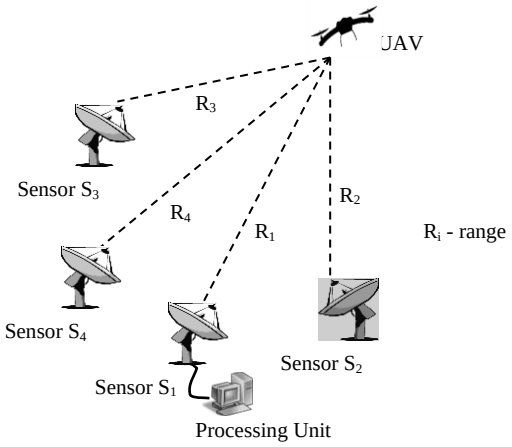

Fig. 4 A typical source localization system

Sensors collect the emitted signal from an unknown radiating source, and signal characteristics like arrival time, received power, the direction of reception, and speed of the signal are used as measurements. The collected measurements are then used in calculating the source position. The sensors (S_1, S_2, S_3, and S_4) collect the emitted radio signals from the unknown radio source/Unmanned Ariel Vehicle (UAV). The choice of measurement technique depends on the geographic and environmental conditions in which the system is placed for operation. The collected measurements are then processed to compute the position by employing any one of the methods, i.e., triangulation, trilateration, or multilateration. The source position is computed concerning a particular receiver or processing system (i.e., system coordinate origin).

In source localization using T.D.O.A. measurements, the sensor which receives the signal first is considered the reference sensor, and T.D.O.A. measurement to other sensors is computed from it. A hyperbola represents the T.D.O.A. measurement between a pair of sensors. As shown in Figure 5, a hyperbola is a locus of points on the plane whose difference in distance to any two fixed points (Foci) on the plane is a constant.

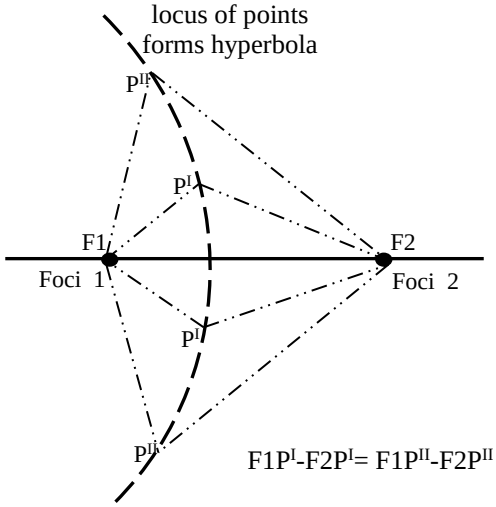

Fig. 5 Hyperbola formation with TDOA/RDOA measurements

This method of source localization using hyperbolas is known as multilateration [4]. T.D.O.A. is considered a superior technique as it overcomes the limitations of the TOA technique. The measurements in T.D.O.A. depend on differences in arrival time of the signal (i.e., independent of source clock) and not on the travel time of the signal; this feature of T.D.O.A. eliminates the necessity of time stamping of the transmitted signal by the source and thereby allows this technique to be suitable for localization of radiating sources [5]. Thus, the clock synchronization problem in the TOA technique has also been addressed by T.D.O.A.; therefore, there is no requirement for the source clock to be time-synchronized with the sensor clock. Hence, when clocks at all the sensors are synchronized, the precision in the T.D.O.A. system is maintained. With the overwhelming advantages of the T.D.O.A. technique, such as signal initiation-time independent measurements, reduced measurement error, and system cost, this technique is widely used for enemy aircraft and source localization on battlefields and in ESM systems, emergency call localization on highways, etc.

The T.D.O.A. measurement of the unknown source signal forms the basis for hyperbolic localization [6,7]. Let the number of sensors required for localization be M. In this work, M = 5. The Range of Arrival (ROA), denoted by R_i is the distance between the unknown radiating source, $\vec{U}(x_u, y_u, z_u)$ to the ith sensor and can be formulated as

$$R_i = \sqrt{(x_i - x_u)^2 + (y_i - y_u)^2 + (z_i - z_u)^2} \qquad (1)$$

where (x_i, y_i, z_i) represent the i^{th} sensor coordinates and i = 1,2,3,4,5.

However, true range information is not available for a source localization system since the time of transmission of the signal from the source is unknown. Only the time of receipt of the signal at a sensor is observed, and the difference in the time of receipt of the signal at two sensors gives the T.D.O.A. value. The Range Difference of Arrival (R.D.O.A.) information can be computed from the T.D.O.A. by multiplying it with the velocity of the signal. $RDOA_{ref,\ i,}$ which is the observed range difference of arrival of the unknown source, $\vec{U}$ between the i^{th} sensor and 'ref,' the reference sensor can be expressed in terms of the ROA in Equation 1 as

$$R.D.O.A._{ref,i} = R_{ref} - R_i \qquad (2)$$

where R_{ref} is the range between the reference sensor $(x_{ref}, y_{ref}, z_{ref})$ And the unknown source.
Therefore, $R.D.O.A._{ref,i}$ is a function of $\vec{U}$ and can be rewritten as

$$R.D.O.A._{ref,i} = \sqrt{(x_{ref} - x_u)^2 + (y_{ref} - y_u)^2 + (z_{ref} - z_u)^2} - \sqrt{(x_i - x_u)^2 + (y_i - y_u)^2 + (z_i - z_u)^2} \qquad (3)$$

where $i \neq ref$.
Equation 2 can be linearized using Taylor's series expansion and approximated to 1st order resulting in

$$\delta \mathrm{RDOA}_{\mathrm{ref,i}} \cong \mathrm{J} \times \delta \vec{\mathrm{U}} \quad (4)$$

where $\delta \mathrm{RDOA}_{\mathrm{ref,i}}$ is the difference between observed and estimated range differences that need to be minimized, i.e., optimized, and J is the Jacobian matrix given by

$$\mathrm{J} = \frac{\partial \mathrm{R.D.O.A._{ref,i}}}{\partial \vec{\mathrm{U}}} \quad (5)$$

If the number of equations and number of unknowns is equal, the unknown variable, $\delta \vec{\mathrm{U}}$ can be evaluated using

$$\delta \vec{\mathrm{U}} \cong \mathrm{J}^{-1} \times \delta \mathrm{RDOA}_{\mathrm{ref,i}} \quad (6)$$

For the over-determined case, $\delta \vec{\mathrm{U}}$ can be evaluated using the update equation of the Gauss-Newton method [5], which is

$$\delta \vec{\mathrm{U}} = (\mathrm{J}^{\mathrm{T}}\mathrm{J})^{-1}\mathrm{J}^{\mathrm{T}} \delta \mathrm{RDOA}_{\mathrm{ref,i}} \quad (7)$$

4. Proposed Iterative Algorithm

The equations that pertain to the collected T.D.O.A. measurements need to be processed for position information. Various algorithms are available for this purpose, like Least Squares, Weighted Least Squares, Gradient Descent, etc. Gauss Newton or Least Squares (L.S.) estimator solves an over-determined system of linear equations obtained from the T.D.O.A. measurement technique in such a way that the resultant solution (position) minimizes the sum of squares of the errors obtained from individual equations. The proposed optimization approach combines the ideas of the Gradient Descent [8] and Gauss-Newton algorithms.

Gradient Descent is an iterative approach in which a direction, $p_{K,}$ is chosen. The algorithm then searches this direction for a lower function value if minimization is the intended result. In this method, the new iteration $\vec{\mathrm{U}}_{\mathrm{K+1}}$ is defined by the direction $p_{K,}$ a function of the objective equation, and by a positive scalar quantity α_{K} called the step length.

$$\vec{\mathrm{U}}_{\mathrm{K+1}} = \vec{\mathrm{U}}_{\mathrm{K}} + \alpha_{\mathrm{K}} p_{\mathrm{K}} \quad (8)$$

The Gauss-Newton method involves inverse computation of the approximated Hessian matrix, Hess = $\mathrm{J}^{\mathrm{T}}\mathrm{J}$ [6, 9]. However, for complex optimization, the matrix, $\mathrm{J}^{\mathrm{T}}\mathrm{J}$ may not be invertible [10]. So that it is invertible, the proposed algorithm introduces an updated Hessian matrix.

$$\mathrm{Hess} = \mathrm{J}^{\mathrm{T}}\mathrm{J} + \mu \mathrm{I} \quad (9)$$

μ, referred to as the combination coefficient, is always positive, and 'I' is an identity matrix of size (M-1×M-1). With this approximation in Equation 9, matrix 'Hess' is always invertible. The update value or error in measurement of the proposed algorithm is given by

$$\delta \vec{\mathrm{U}} = (\mathrm{J}^{\mathrm{T}}\mathrm{J} + \mu \mathrm{I})^{-1}\mathrm{J}^{\mathrm{T}} \delta \mathrm{RDOA}_{\mathrm{ref,i}} \quad (10)$$

The update value in Equation 10 switches between Equation 7 and 8 during the sensor position estimation. When the combination coefficient denoted by μ is very small (close to zero), Equation 10 approaches Equation 7, and the least-squares method is used. When μ is very large, Equation 10 approaches the updated value in Equation 8, and the gradient descent method is used (with $\alpha_K \cong {}^{1}/_{\mu}$).

5. Working Methodology

The entire coding process has been done in M.A.T.L.A.B. The proposed algorithm is evaluated for a radiating source in the near and far fields of the sensor configuration. Sensor geometry is one of the major factors that affect the accuracy of a localization system, independent of any measurement errors. This effect of source-sensor geometry on localization accuracy is called G.D.O.P. and can be expressed utilizing the G.D.O.P. coefficient. In addition, statistical accuracy measures like Circular Error Probable (C.E.P.) can be used to characterize the effect of geometrical considerations on localization. Sensors can be arranged in any number of geometries for localization. An object is said to be in the near field of any sensor geometry if its distance from the reference origin is less than or of the order of the maximum distance between the reference sensor and other sensors. Also, a source is said to be in the far-field of any sensor geometry if its distance from the reference origin exceeds four times the maximum distance between the reference sensor and other sensors [11]. Accordingly, all the sensor and source locations have been chosen [12, 13]. The sensors are in square geometry, with the reference sensor positioned at the center of the arrangement, as shown in Figure 6.

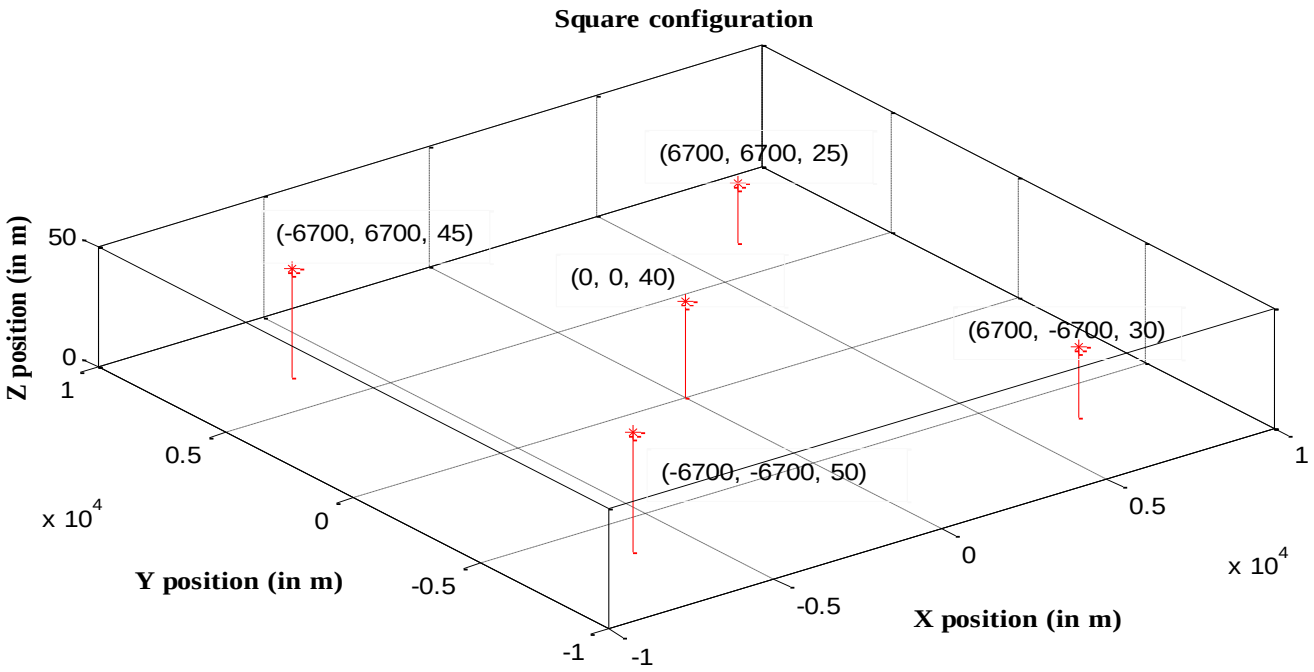

Fig. 6 Sensors arranged in Square configuration

5.1. Generation of C.E.P. profile

To opt for the best sensor geometry from among a set of choices, C.E.P. is the statistical accuracy measure used for evaluation. The value of C.E.P. varies with the geometry of the sensor position(s) and the unknown source, the variances for the measured parameters, and the number of measurements. Some sensor geometries were considered for evaluation, and C.E.P. profiles were generated for each geometrical configuration. The C.E.P. profile for the sensors located in square geometry, which has been identified as the best possible arrangement of sensors, is shown in Figure 7.

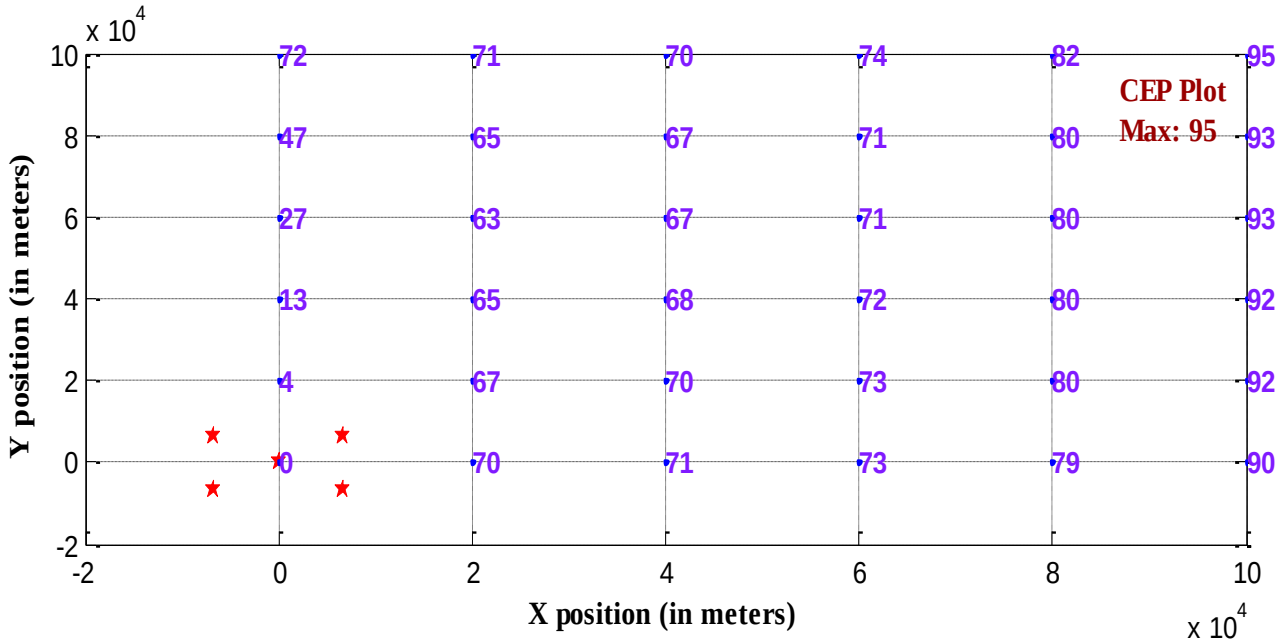

Fig. 7 C.E.P. profile for Square geometry

- The chosen sensor geometry is considered for evaluation.
- The unknown source x and y-positions are varied from 0 to 100 km in steps of 20 km each, thus creating a total survey area of 10000 sq. kms. The height of the source is, however, fixed at 7kms. Thus, a total of 36 source locations (with (X, Y) = (0, 0), (0, 20 km)…. (100 km, 100kms)) are evaluated for each sensor geometry.

- For each of the 36 source locations, the range difference of arrival (R.D.O.A.) values are calculated. Four T.D.O.A. (or R.D.O.A.) values are used to estimate source position since 5 sensors are assumed to be available.
- Random Gaussian noise varying from 0 to 6ns is added to all the four T.D.O.A. values (1ns error in T.D.O.A. corresponds to an error of 0.3m in R.D.O.A.).
- To ensure that the entire error range, i.e., 0 to 6ns, is covered, 1000 different error combinations of the four T.D.O.A. values are considered. Hence, 1000 sets of the four T.D.O.A.s are generated.
- The unknown source position is estimated using the proposed iterative algorithm for each combination of the set of T.D.O.A.s. Thus, 1000 estimations are generated for each of the 36 locations.
- The variances of the measured parameters (X and Y positions of all 1000 estimations) are obtained for each location.
- The C.E.P. value for each location is calculated.

Once the C.E.P. value is calculated for all 36 source locations, the C.E.P. profile is generated for the chosen sensor geometry. This process is repeated for all the seven sensor geometries. C.E.P. values are low when the source location is closest to the sensor geometry. The maximum C.E.P. for the Square geometry is obtained at the source location (100km, 100km) and is equal to 95m.

5.2. Determination of the G.D.O.P. profile

Similarly, the G.D.O.P. profile for the chosen sensor configuration can also be calculated. The T.D.O.A. measurement equation can be linearized and approximated using 1st order Taylor's series [4]. The resultant linearized equation is given by Equation 11.

$$J \times \delta\vec{U} = \delta\vec{R}DOA \tag{11}$$

Localization accuracy is defined as the degree of closeness of the true position to the estimated position [14] or as the error in the estimated position [15]. It depends primarily on measurement error and sensor geometry. This relationship can be described by

$$\text{Estimated source location Accuracy} = \text{Sensor to source geometry} \times \text{UERE} \tag{12}$$

where U.E.R.E. denotes User Estimated Range Error or Root Mean Square Error in range (R.M.S.E.).

For T.D.O.A. systems, the U.E.R.E. term in Equation 12 is the vector, δRDOA, which denotes error in range (R.D.O.A.) measurements. The measurement and position errors are generally considered random variables with zero mean and variance equal to unity (i.e., standard normal distribution). Hence, their R.M.S.E. is calculated from error covariance matrices, and Equation 12 is modified as given in Equation 13.

$$Location\ Accuracy = Geometry \times trace\{E\left[\left(\delta RDOA_i - E(\delta RDOA_i)\right)\left(\delta RDOA_i - E(\delta RDOA_i)\right)^T\right]\} \tag{13}$$

It is evident from Equation 12 that even though the measurements are not uncertain (i.e., UERE=Identity Matrix), position accuracy is affected by geometry. G.D.O.P. is defined as the coefficient that explains the effect of source sensor geometry on the relationship between R.M.S.E. in measurements, δRDOA to R.M.S.E. in position estimate, δU. It is implied that the computation of G.D.O.P. determines the effect of the sensor geometry on position accuracy, δU. The term $COV_{\delta U}$ in Equation 14 represents the position error covariance matrix.

$$COV_{\delta U} = E\left(\left(\delta U - E(\delta U)\right)\left(\delta U - E(\delta U)\right)^T\right) \tag{14}$$

Here, E is the mean operator or expectation, and on the assumption that the mean of the position error is zero, Equation 13 can be written as

$$COV_{\delta U} = E\left(\left(\delta U\right)\left(\delta U\right)^T\right) \tag{15}$$

On substituting Equation 14 in 15, the Covariance matrix is given by

$$COV_{\delta U} = E\left(\left((J^TJ)^{-1}J^T\delta\vec{R}DOA\right)\left((J^TJ)^{-1}J^T\delta\vec{R}DOA\right)^T\right)$$
$$COV_{\delta U} = E\left((J^TJ)^{-1}J^T\delta\vec{R}DOA\,\delta\vec{R}DOA^T\left((J^TJ)^{-1}J^T\right)^T\right) \tag{16}$$

As the elements present in matrix B are measured values, the expectation operator is applied only to the measurement error matrix, and Equation 16 is represented as

$$COV_{\delta U} = (J^TJ)^{-1}J^T\left((J^TJ)^{-1}J^T\right)^T E\left(\delta\vec{R}DOA\,\delta\vec{R}DOA^T\right) \tag{17}$$

Here, the measurement error covariance matrix, $COV_{\delta RDOA}$ is represented by $E\left(\delta RDOA.\delta RDOA^T\right)$ With an assumption that the measurement error mean is zero. It is obvious from Equation 11 that the Jacobian, J is the only matrix that contains the information of source sensor geometry and therefore is also referred to as the geometry matrix. For further simplification, Equation 17 can be rewritten as

$$COV_{\delta U} = \left((J^TJ)^{-1}\right)COV_{\delta\vec{R}DOA} = \left((J^TJ)^{-1}\right)E\left(\delta\vec{R}DOA\,\delta\vec{R}DOA^T\right)$$
$$\because (J^TJ)^{-1}\left(J^TJ\right) = I \tag{18}$$

For the considered source localization system, the size of matrix J in Equation 11 is 4x3, and the resultant matrix in Equation 18 $(J^{T.J.})^{-1}$ is a 3x3 square matrix. The G.D.O.P. coefficient is defined by the trace of this matrix, with the diagonal elements providing the estimated position error variances [16,17].

The Coefficient of G.D.O.P. can be calculated as [18]

$$GDOP = \text{trace}\left((J^T J)^{-1}\right) = \sqrt{Var_X + Var_Y + Var_Z}$$

$$\text{Where } \left((J^T J)^{-1}\right) = \begin{bmatrix} Var_X & Cov_{XY} & Cov_{XZ} \\ Cov_{YX} & Var_Y & Cov_{YZ} \\ Cov_{ZX} & Cov_{ZY} & Var_Z \end{bmatrix}$$

Figure 8 depicts the G.D.O.P. profile for the Square geometry. The value of G.D.O.P. for each source is indicated at the corresponding source location. It can be observed that the G.D.O.P. increases with an increase in the distance of the source from the sensor geometry. The maximum G.D.O.P. is obtained at the source location (0, 100 km) and is equal to 719.

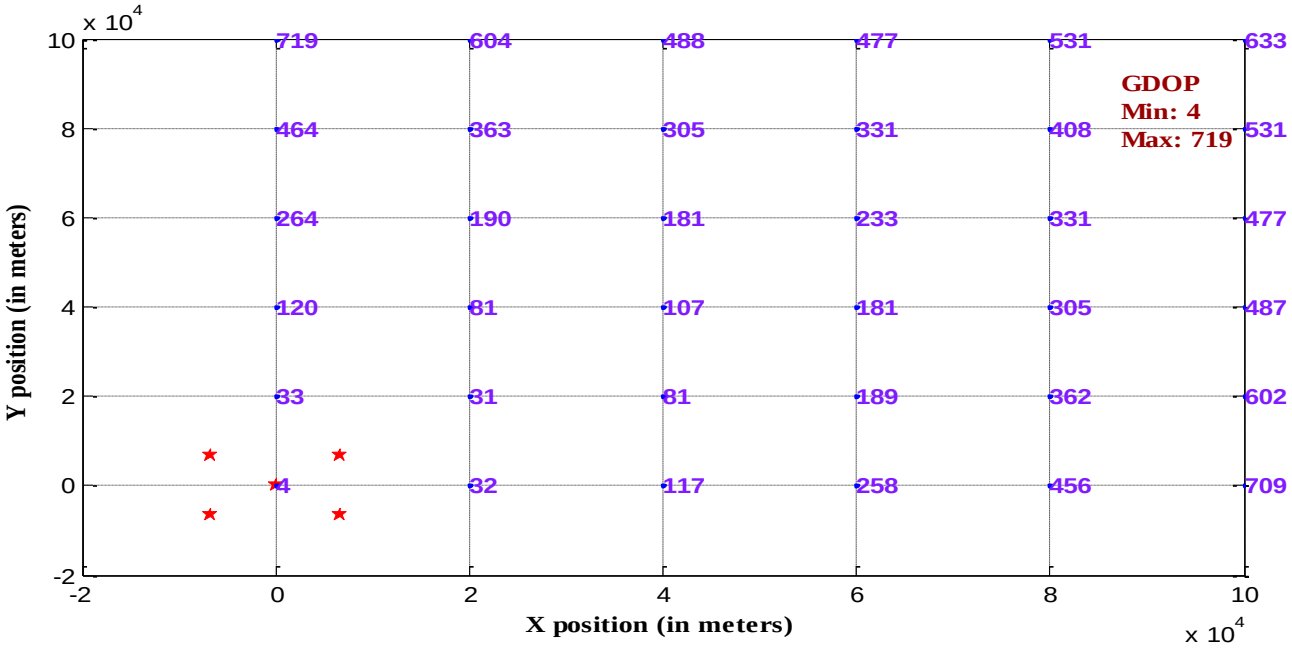

Fig. 8 G.D.O.P. profile for Square geometry

Figure 9 sketches the G.D.O.P. contour plot corresponding to Figure 8. The contour plot helps identify how the geometry affects source locations distributed over the survey area. The D.O.P. values increase with an increase in the distance of the source from the geometry.

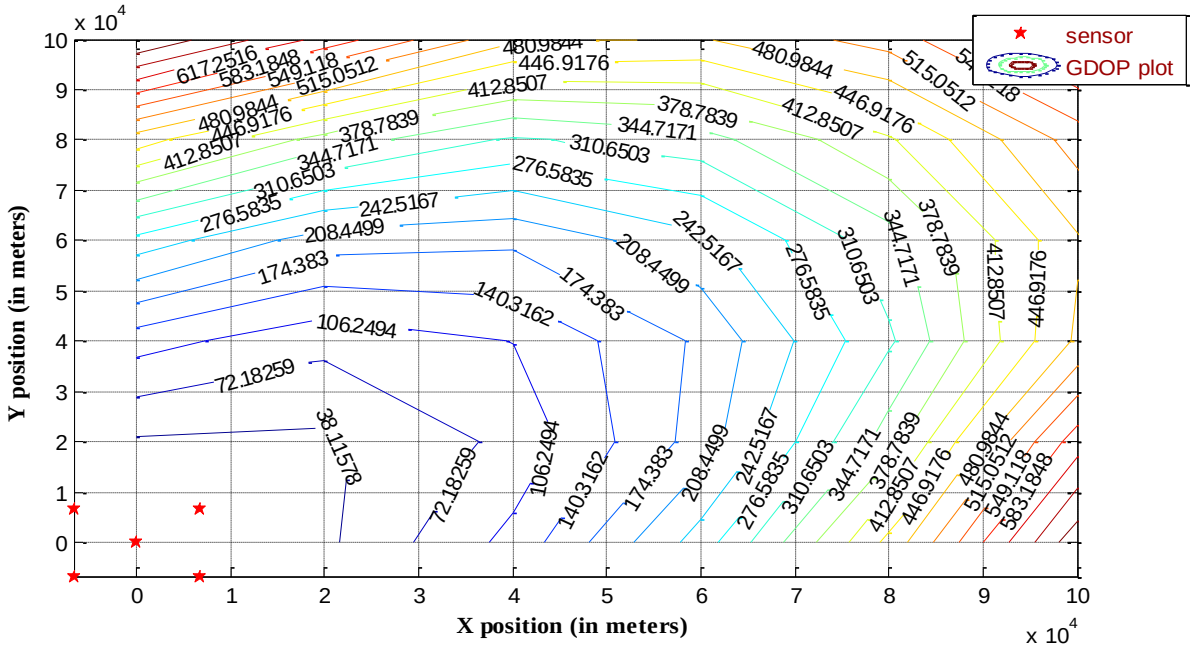

Fig. 9 G.D.O.P. contour plot for Square geometry

5.3. Computation of Localization solution

The maximum distance between sensors is about 19 km. For the far-field case, the source is positioned at a distance of 100 km from the reference origin and a height of 7 km. For the near field case, the source is positioned at a distance greater than 19 km from the reference origin and at the height of 2 km. The assumed true location of the far source is (x, y, z) = (60 km, 80 km, 7 km). Assumed true location of near-source (x, y, z) = (18 km, 7 km, 2 km). The following process is carried out in computing localization solutions using the proposed iterative method.

1) Collect the range difference measurements $\mathrm{RDOA}_{1,2}, \mathrm{RDOA}_{1,3}, \mathrm{RDOA}_{1,4}$ and $\mathrm{RDOA}_{1,5}$ from 5 sensors with sensor 1 as reference.
2) Initialize the source position vector, $\overrightarrow{U_k} = [\mathrm{x_{uK}}, \mathrm{y_{uK}}, \mathrm{z_{uK}}]^T$ and combination coefficient, μ.
3) Compute the range difference measurements $\mathrm{R.D.O.A._{1,2k}}$, $\mathrm{R.D.O.A._{1,3k}}$, $\mathrm{R.D.O.A._{1,4k}}$ and $\mathrm{R.D.O.A._{1,5k}}$ using the source position guess in step 2.
4) Calculate the error in the measurement vector from steps 1 and 3. $\delta\vec{\mathrm{R}}\mathrm{DOA} = [\delta\mathrm{RDOA}_1\ \delta\mathrm{RDOA}_1\ \delta\mathrm{RDOA}_1\ \delta\mathrm{RDOA}_1]^{\mathrm{T}}$
5) Compute, $\mathrm{E_0} = (\delta\vec{\mathrm{R}}\mathrm{D.O.A.}^{\mathrm{T}}\ \delta\vec{\mathrm{R}}\mathrm{D.O.A.})$ from step 4.
6) Calculate the Jacobian matrix, $\mathrm{J_{M\text{-}1\times3,}}$ and the Hessian matrix, $\mathrm{Hess} = \mathrm{J^TJ}$
7) Determine the updated value or change in position $\delta\vec{\mathrm{U}} = [\delta\mathrm{x_u}\ \delta\mathrm{y_u}\ \delta\mathrm{z_u}]^{\mathrm{T}}$ with (10).
8) Update the source position vector in Step 2 with the change in position vector obtained in Step 7. (i.e.$\vec{\mathrm{U}}_{\mathrm{K+1}} = \vec{\mathrm{U}}_{\mathrm{K}} + \delta\vec{\mathrm{U}}$)
9) Repeat step 3 with the updated position in step 8.
10) Calculate the error in measurement vector $\delta\vec{\mathrm{R}}\mathrm{D.O.A.}$ from steps 1 and 9.
11) Compute $\mathrm{E_1} = (\delta\vec{\mathrm{R}}\mathrm{D.O.A.}^{\mathrm{T}}\ \delta\vec{\mathrm{R}}\mathrm{D.O.A.})$ from step 10.
12) Compare $\mathrm{E_0}$ and $\mathrm{E_1}$. If $\mathrm{E_0} > \mathrm{E_1}$, update the combination coefficient using $\mu = \mu/10$ in (10), assign $\vec{\mathrm{U}}_{\mathrm{K}} = \vec{\mathrm{U}}_{\mathrm{K+1}}, \mathrm{E_0} = \mathrm{E_1}$ and repeat steps 6 to 12. Else update the combination coefficient using $\mu = \mu \times 10$ in (10) and repeat steps 7 to 12.
13) Repeat Steps from 6 to 12 for a fixed number of iterations or until a threshold criterion is satisfied.

$\vec{\mathrm{U}}_{\mathrm{K+1}} = [\mathrm{x_{uK+1}}, \mathrm{y_{uK+1}}, \mathrm{z_{uK+1}}]^T$ is the final source position estimate.

5.4. Evaluation of the proposed algorithm

The steps for evaluating the proposed algorithm are as follows:

- The algorithm must be evaluated for the unknown source location in either the near or far-field of the chosen square geometry of sensors. Hence, one of the two cases is considered.
- The true range difference of arrival (R.D.O.A.) values for the chosen source location are calculated. Four T.D.O.A. (or R.D.O.A.) values are used to estimate source location since 5 sensors are available.
- Random noise between 0 and 6ns is added to all the four T.D.O.A. values. To ensure that the entire error range, i.e., 0 to 6ns, is covered, 1000 different error combinations are generated. Each combination consists of four random values between 0 and 6 ns. They are added to the four true T.D.O.A. values to approximate real-time data. Hence, 1000 Monte Carlo sets of the four observed T.D.O.A.s are generated.
- The unknown source location is estimated using the proposed algorithm for each combination of the set of T.D.O.A.s, generating a total of 1000 estimations.
- The mean and variance of the estimated parameters (x, y, and z coordinates of all 1000 estimations) are obtained.

The error scatters plot comparing errors in estimated x, y, and z locations are generated to conduct an error analysis of the chosen algorithm. Statistical accuracy measures like C.E.P. and Twice Distance Root Mean Square (2DRMS) give an idea of the position accuracy of the algorithm used. 2DRMS is twice the R.M.S. of the horizontal errors. C.E.P. is defined as the circle's radius centered on the source within which the impact probability is 0.5 [19]. The estimated parameters are the unknown source location coordinates, i.e., x and y. There are several methods to estimate CEP [20,21,22,23]. The approximated expression used for C.E.P. [24] is

$$CEP = 0.614\sigma_X + 0.563\sigma_Y$$

Here σ_X and σ_Y are the standard deviations of the estimated x and y distances from the mean of the estimates, respectively. Similar to the 2D accuracy measures, many representations of 3D accuracy have various probabilities. 3D accuracy measures are conceptually similar to those in 2D expanded by one more dimension, i.e., the vertical accuracy. Spherical Error Probable (S.E.P.) corresponds to C.E.P. in 2D, while Mean Radial Spherical Error (M.R.S.E.) corresponds to DRMS in 2D. The 99% spherical accuracy standard is the sphere's radius centered at the true position, containing the estimated position in 3D with a probability of 99%.

6. Results and Analysis

Figure 10 shows errors in X, Y, and Z location coordinates estimated using the proposed algorithm for far source. A small sample of estimated source positions and errors in estimations for five different error combinations is tabulated in Table 1 from among 1000 error combinations. The following observations can be made. The mean error in X, Y, and Z due to the Gauss-Newton and the proposed iterative algorithms for far source are μ_X =61.6m, μ_Y =81.98m, μ_Z =83.40m, and μ_X =61.3m, μ_Y =81.86m, μ_Z = 85.07m respectively. The corresponding uncertainties observed are σ_X=45.32m, σ_Y =60.43m, σ_Z =30.23m and σ_X=44.83m, σ_Y =59.76m, σ_Z =30.29m respectively. The proposed algorithm performs better when compared to the Gauss-Newton algorithm though the difference in performance is not considerable. However, the latter algorithm faces the problem of dependence on an initial guess, which is not the case with the proposed algorithm.

The Gradient Descent algorithm is out of contention since it consumes a large number of iterations and hence a lot of time.

Figure 11 illustrates the location error scatter plot of the proposed algorithm with C.E.P. and 2DRMS circles indicated. The corresponding C.E.P. and 2DRMS are 61.2m and 149.4m, respectively, for the proposed iterative algorithm. The ratio of C.E.P. to the distance of the far source from the reference origin is 0.0006. Figure 12 shows estimates for the near-source. A small sample of these estimations is presented in Table 2. The mean error in X, Y, and Z due to the Gauss-Newton and the proposed iterative algorithms for near-source are μ_X =4.43m, μ_Y =2.17m, μ_Z =9.39m, and μ_X =4.40m, μ_Y=2.14m, μ_Z = 9.20m respectively. The corresponding uncertainties observed are σ_X =3.33m, σ_Y =1.57m, σ_Z =5.58m and σ_X =3.27m, σ_Y =1.55m, σ_Z =5.56m respectively. The corresponding C.E.P. and 2DRMS are 2.9m and 7.25m, respectively, as shown in Figure 13. The ratio of C.E.P. to the distance of the near-source from the reference origin is approximately 0.00015.

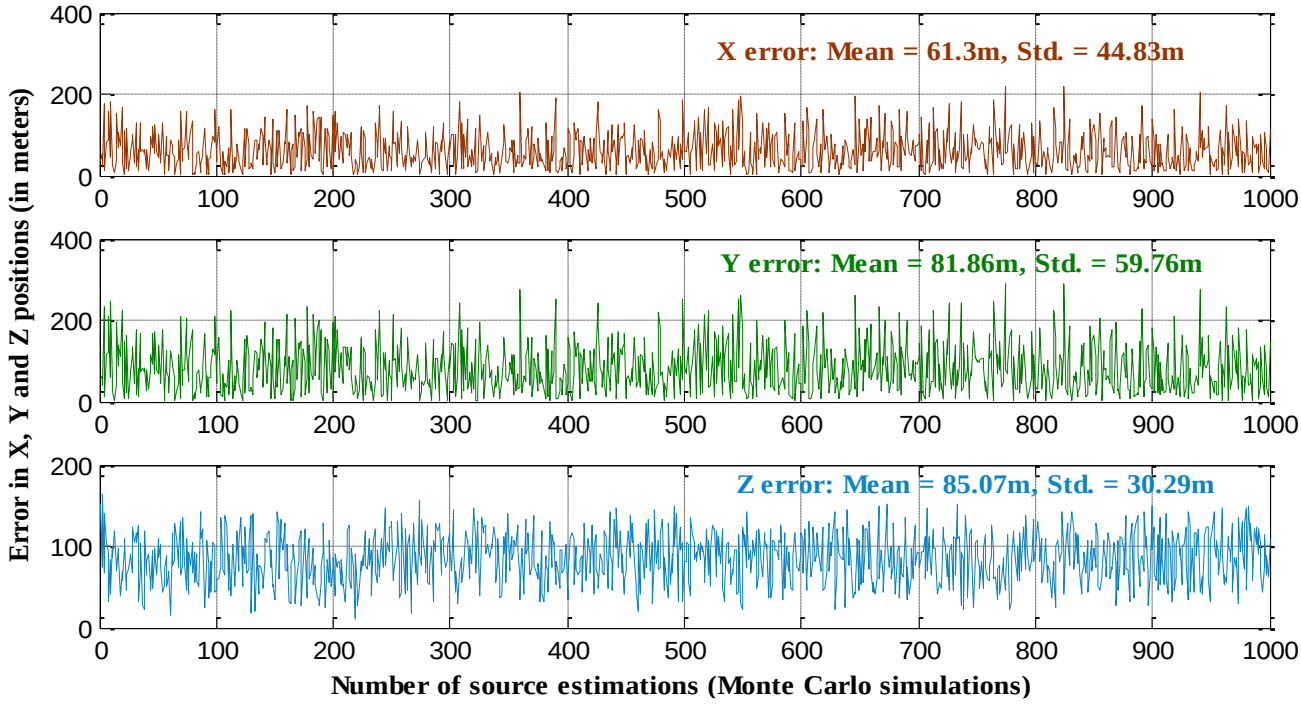

Fig. 10 Error in X, Y, and Z for far source estimations

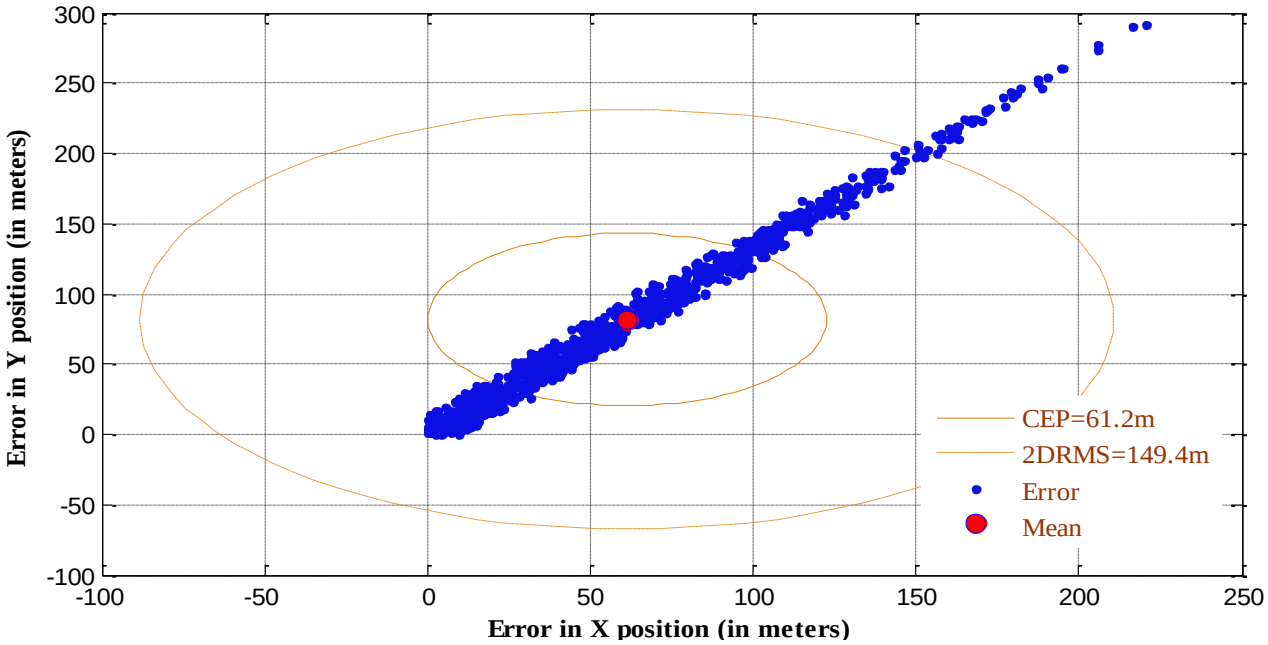

Fig. 11 Horizontal location error scatter plot for far source

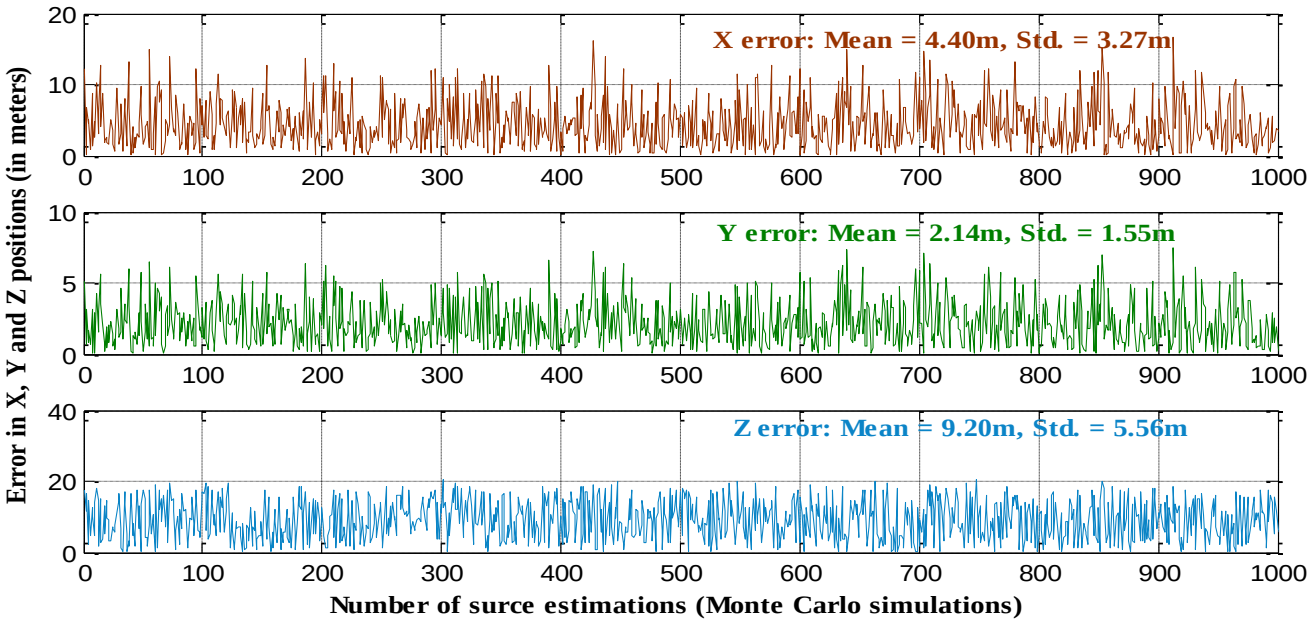

Fig. 12 Error in X, Y, and Z for near-source estimations

A comparison of the various 2D and 3D accuracy measures calculated for the proposed iterative algorithm is presented in Table 3 for both the near and far source cases. The results presented in Table 3 indicate uniformity among the different accuracy measures for both near and far source cases. The difference between C.E.P. and S.E.P. is also marginal for the chosen altitude values of the source. Also, to compare the performance of the proposed algorithm with the Gauss-Newton method, it is pertinent that the accuracy measures of the latter should also be analysed. The values of C.E.P. and 2DRMS for the Gauss-Newton algorithm for far source are 61.94m and 151.08m, respectively. The corresponding values of C.E.P. and 2DRMS for the near-source are 2.94m and 7.37m, respectively. An immediate comparison with the values obtained for the proposed algorithm verifies the improvement obtained.

Table 1. Error in source position due to proposed algorithm for far source

SNo	T.D.O.A. 1 Error (ns)	T.D.O.A. 2 Error (ns)	T.D.O.A. 3 Error (ns)	T.D.O.A. 4 Error (ns)	Estimated Source position in meters			Error in estimation in meters		
					X pos	Y pos	Z pos	X pos	Y pos	Z pos
1	4.56	1.75	1.66	0.04	60115.9	80146.7	7041.2	115.9	146.79	41.20
2	2.25	2.62	1.83	1.75	60026.3	80034.8	7059.0	26.38	34.80	59.02
3	1.46	5.62	5.16	2.38	60030.1	80051.2	7086.1	30.12	51.23	86.11
4	2.88	3.39	2.94	1.62	60056.4	80076.0	7066.6	56.40	76.08	66.67
5	5.94	1.10	5.17	0.20	60220.4	80291.3	7045.0	220.4	291.39	45.06
Mean (in m)					60039	80053	7085.1	61.30	81.86	85.07
Standard deviation (σ) (in m)					64.99	86.12	30.29	44.83	59.76	30.29
Variance (σ^2) (in Sq.m)					4224.9	7417.6	917.73	2010	3571.5	917.7

Table 2. Error in source position due to proposed algorithm for far source

SNo	T.D.O.A. 1 Error (ns)	T.D.O.A. 2 Error (ns)	T.D.O.A. 3 Error (ns)	T.D.O.A. 4 Error (ns)	Estimated Source position in meters			Error in estimation in meters		
					X pos	Y pos	Z pos	X pos	Y pos	Z pos
1	0.35	0.72	0.78	4.82	17994.7	6997.5	2003.5	5.26	2.47	3.49
2	0.96	3.15	4.25	5.94	17995.7	6998.7	2013.8	4.28	1.32	13.81
3	3.66	1.75	3.31	3.24	18004.2	7001.4	2011.0	4.21	1.44	10.99
4	5.40	0.43	5.90	5.43	18011.0	7004.7	2020.6	10.97	4.67	20.58
5	3.50	2.35	3.35	5.92	17999.7	6999.3	2011.5	0.29	0.66	11.54
Mean (in m)					18001	6999.9	2009.2	4.40	2.14	9.20
Standard deviation (σ) (in m)					5.46	2.64	5.63	3.27	1.55	5.56
Variance (σ^2) (in Sq.m)					29.86	6.99	31.70	10.73	2.41	31.01

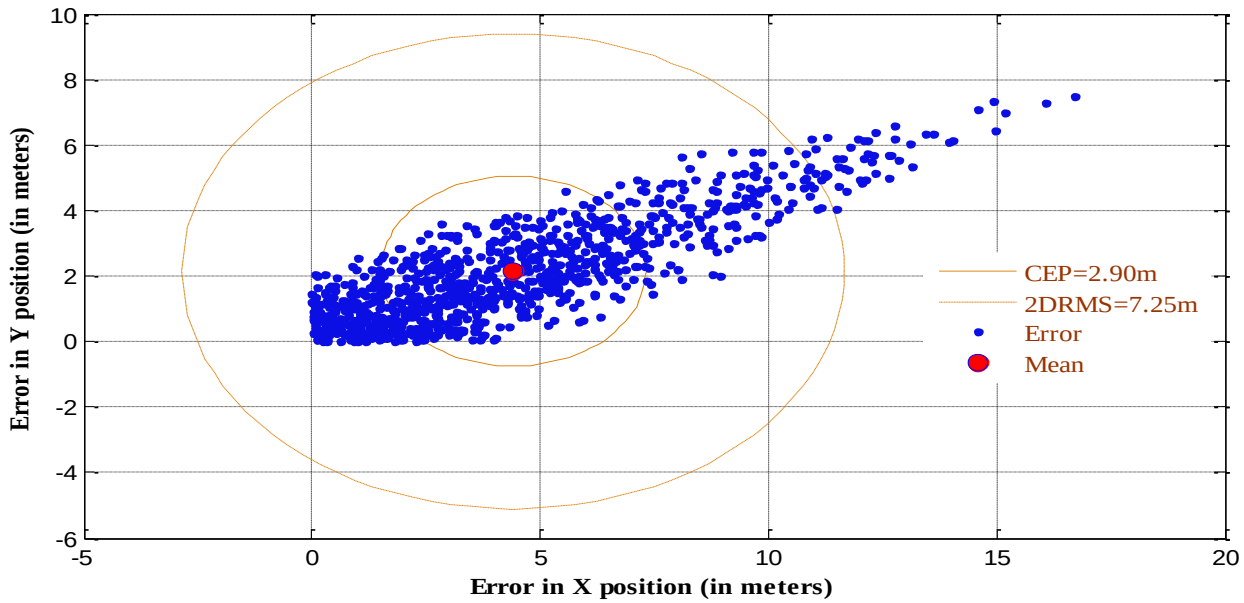

Fig. 13 Horizontal location error scatter plot for near-source

Table 3. Comparison of Accuracy Measures for the proposed algorithm

Statistical Accuracy Measures for Proposed Algorithm		Far Source	Near Source
2D accuracy in m (Horizontal)	CEP (50%)	61.26	2.9
	2DRMS (95%)	149.42	7.25
3D accuracy in m (Horizontal & Vertical)	SEP (50%)	68.79	5.3
	MRSE (61%)	80.62	6.64
	SAS (99%)	151.35	11.66

7. Conclusion

In this paper, the proposed iterative algorithm was characterized using C.E.P. and other statistical accuracy measures providing useful knowledge of the change in expected localization error with distance. An initial observation suggests that the algorithm's performance worsens with the increase in the distance of the source. The C.E.P. and 2DRMS values for the near-source are 2.9m and 7.25m, while those for the far source are 61.2m and 149.4m, respectively. However, comparing the ratios of C.E.P. to the source distance for both the near (0.00015) and far (0.0006) cases indicates that the performance doesn't deteriorate much for the chosen sensor geometry. The marginal difference in error between 2D and 3D accuracy measures can be attributed to the algorithm's superior performance in resolving the altitudinal information of the unknown source.

Conflict of Interest

The author(s) declare(s) that there is no conflict of interest regarding the publication of this paper.

References

[1] Electronic Warfare, Global Defence Technology Digital Magazine - Special Issue, May (2018).

[2] Long Cheng, Cheng dong Wu, Yunzhou Zhang, Hao Wu, Mengxin Li and Carsten Maple, A Survey of Localization in Wireless Sensor Network, International Journal of Distributed Sensor Networks, Hindawi Publishing Corporation, Article ID: 962523, 8(12) (2012).

[3] Laveti, G., Eswara Chaitanya, D., Chaya Devi, P., Vinodh Kumar, T. Positioning Strategies: Implementation and Applications of Major Source Localization and Positioning Approaches Over Indian Subcontinent. In: Chowdary, P., Chakravarthy, V., Anguera, J., Satapathy, S., Bhateja, V. (eds) Microelectronics, Electromagnetics and Telecommunications. Lecture Notes in Electrical Engineering, 655(2021). Springer, Singapore. https://doi.org/10.1007/978-981-15-3828-5_22.

[4] Eswara Chaitanya D., Kumar M.N.V.S.S., Sasibhushana Rao G. and Rajkumar Goswami, Convergence Issues of Taylor Series Method in Determining Unknown Target Location Using Hyperbolic Multilateration, I.C.S.E.M.R. (2014), ISBN:978-1-4799-7613-3/14/IEEE-2014.

[5] Homayun Kabir, Jeevan Kanesan, Ahmed Wasif Reza, Harikrishnan Ramiah, A Mathematical Algorithm of Locomotive Source Localization Based on Hyperbolic Technique, International Journal of Distributed Sensor Networks, Hindawi Publishing Corporation, Article ID: 384180, 2015(2015).

[6] Levenberg Kenneth, A Method for the Solution of Certain Nonlinear Problems in Least Squares, Quarterly of Applied Mathematics, 2(2) (1944) 164–168.

[7] B. T. Fang, Simple Solutions for Hyperbolic and Related Position Fixes, IEEE Transactions on Aerospace and Electronic Systems, 26(5) (1990) 748- 753.
[8] R. Zekavat and R. Buehrer, Source Localization: Algorithms and Analysis, in Handbook of Position Location:Theory, Practice and Advances , 1, Wiley-IEEE Press, (2012).
[9] Richard Szeliski, Computer Vision Algorithms and Applications, Springer, ISBN: 1868-0941, London, (2011).
[10] Bogdan M.Wilamowski, J. David Irwin, The Industrial electronics Handbook, Intelligent Systems, 2nd ed, C.R.C. Press, 2011.
[11] Richard J. Barton and Divya Rao, Performance Capabilities of Long-Range UWB-IR TDOA Localization Systems, E.U.R.A.S.I.P. Journal on Advances in Signal Processing, (2007).
[12] Report of The Fourteenth Meeting of the Regional Airspace Safety Monitoring Advisory Group (R.A.S.M.A.G./14), International Civil Aviation Organization, Bangkok, Thailand, 21-25 February, (2011).
[13] (2011) J.A.S.M.A. website. [Online]. Available: http://www.jasma.jp/height-monitoring.html
[14] NovAtel, APN-029, Statistics and its relationship to accuracy measure in G.P.S., Rev-1, (2003) 1-6.
[15] Catherine A. Peters, Statistics for Analysis of Experimental data, Environmental Engineering Processes Laboratory Manual-2001.
[16] Guoqiang Mao, Baris Fidan, Localization Algorithms and Strategies for Wireless Sensor Networks, Information Science reference, New York, (2009).
[17] Dudek, Gregory; Jenkin, Michael (2000), Computational Principles of Mobile Robotics, Cambridge University Press. ISBN 0-521-56876-5.
[18] G. Laveti, G. S. Rao, D. E. Chaitanya et al., T.D.O.A. measurement based G.D.O.P. analysis for radio source localization, Procedia Computer Science, 85 (2016) 740-747.
[19] C. McMillan & P. McMillan, Characterizing rifle performance using circular error probable measured via a flatbed scanner, (2008).
[20] Blischke, W. R.; Halpin, A. H. Asymptotic Properties of Some Estimators of Quantiles of Circular Error. Journal of the American Statistical Association. 61 (315) (1966) 618–632.
[21] Spall, James C.; Maryak, John L. A Feasible Bayesian Estimator of Quantiles for Projectile Accuracy from Non-iid Data. Journal of the American Statistical Association. 87 (419) (1992) 676–681.
[22] Winkler, V. and Bickert, B. Estimation of the circular error probability for a Doppler-Beam-Sharpening-Radar-Mode, in E.U.S.A.R. 9th European Conference on Synthetic Aperture Radar, 368–71, 23/26 (2012).
[23] Mario Ignagni, Determination of Circular and Spherical Position-Error Bounds in System Performance Analysis, Journal of Guidance, Control, and Dynamics, 10.2514/1.47573, 33(4) (1301-1305) (2010).
[24] J. T. Gillis, Computation of the circular error probability integral, IEEE Transactions on Aerospace and Electronic Systems, 27(6) (1991) 906-910.